

State Feedback Via Judicious Pole Placement and Linear Quadratic Regulator – Application to Rotary Inverted Pendulum

Muhammad Nizam Kamarudin^{1*}, Rozilawati Mohd Nor¹, Sahazati Md Rozali¹, Mohd Saifuzam Jamri¹

¹ Center for Robotics and Industrial Automation (CeRIA), Faculty of Electrical Technology and Engineering, Universiti Teknikal Malaysia Melaka, Hang Tuah Jaya, 76100 Durian Tunggal, Melaka, MALAYSIA

*Corresponding Author: nizamkamarudin@utem.edu.my

DOI: <https://doi.org/10.30880/ijie.2024.16.05.001>

Article Info

Received: 4 December 2023

Accepted: 15 May 2024

Available online: 1 August 2024

Keywords

State feedback, linear quadratic regulator, rotary inverted pendulum

Abstract

In the control system regulatory concept, placing closed loop poles too far from the origin in the stability region produces fast regulation time but requires huge forcing energy as a trade-off. As such, stabilizing an unstable system with minimum energy is needed, though this presents a challenge to the designer. At the design phase, the designer may ponder the optimized energy while compromising the possibility of catastrophic stabilization phenomena due to minimal forcing thrust towards the poles. In this manuscript, a simple Linear Quadratic Regulator (LQR) is proposed as an alternative to full state feedback (FSF) with judicious pole placement. The efficacy of both approaches was observed by exploiting a Rotary Inverted Pendulum (RIP) as a testbed. Beforehand, the RIP system dynamics were developed in the time domain. RIP is an under-actuated mechanical system that is inherently nonlinear and unstable. The main control objectives of RIP are swing-up control, stabilization control, switching control, and trajectory control. The methodology involved the appearance of weighted matrices that were necessary for the minimum cost function. The Riccati and Lyapunov criteria are also exploited to facilitate design. The result shows the comparative transient performances of the two approaches, where the LQR outperforms the FSF in many aspects.

1. Introduction

It is effortless to stabilize unstable systems by forcing their poles to the left-hand side of the S -plane so that the closed-loop system is stable. Theoretically, placing the closed-loop poles approaching $-\infty$ may result in a fast regulation rate but require high energy as a trade-off. For instance, consider a linear system $\dot{x}=Ax+Bu$ where x is the state, A denotes a system matrix, B is the input matrix and u be the control input. By the pole placement approach, state x can be regulated to equilibrium $x=0$ by a simple state feedback control law $u=-Kx$. Without considering the magnitude and amount of energy in the control signal u , the designer will ponder the satisfactory value for the feedback gain K such that the closed loop system $\dot{x}=(A-BK)x$ stable. For this motive, the designer may simply choose any K so that the eigenvalues of a new system matrix $(A-BK)$ positioned at the left-hand side of the S -plane. However, formulating the gain K by placing a pole via trial-and-error results in a few shortcomings. Often, the stabilization rates are the performance to be improved without considering the energy to be used by the control effort while forcing the poles to a desired location. Surprisingly, pole placement via trial-and-error has been widely used to date [1,2]. In [1], a DC motor system is stabilized by a feedback gain obtained via trial pole location. The author in [2] obtained the feedback gain via simple MATLAB coding that is

This is an open access article under the CC BY-NC-SA 4.0 license.



developed to stabilize a 3rd-order linear-time-invariant (LTI) system. A more advanced pole placement approach is reported in [3] where the direct adaptive learning-based tuning strategy was exploited for a reasonable pole location. In a state-observer-based control [4], the error feedback to a regulator is measured based on the observer output rather than the actual states. The estimated states that are fed back to the regulator are stabilized in the same manner as in the actual state such that the previously mentioned closed loop matrix $(A-BK)$ becomes positive definite. In the above-mentioned literature [1,2,3,4] and all literature therein, the control effort is neither presented nor recorded. As such, it is difficult to monitor the amount of energy being injected into the system when the stabilization takes place.

To achieve the boundedness of control energy, a few advanced and complicated techniques are proposed. To name a few, a well-established classical approach to avoiding excessive control signals is the anti-windup scheme [5,6,7]. Principally, the anti-windup compensator is augmented with the nominal controller to avoid an integral term from windup during control input saturation. An obvious shortcoming of this approach is that the analysis of a standard anti-windup design reveals a strongly limited region of attraction because the amount of the required control signal has been cut off before it enters the system under control. The technique also requires advanced mathematics and is not optimal. Achieving the same result via non-trivial cum no-complex design gives advantages to the designer. In this manuscript, an optimal design based on the minimum performance index is the suggested technique to be pondered. Among many available state feedback optimal techniques ranging from a minimum time problem [8], minimum energy problem [9, 10] and a state regulation problem [11], a linear quadratic regulation problem [12, 13] has been chosen because it combines state regulation with a minimum energy optimization. As such, regulation takes place through two positive-definite weighted matrices.

To observe the effectiveness and efficacy of the technique, a Rotary Inverted Pendulum (RIP) is used as a testbed. RIP is an under-actuated mechanical system that is inherently non-linear and unstable. For decades, it has been used as a testbed to observe the controller's performance and efficacy. Numerous control studies on RIP were presented in [14-22]. The modeling and dynamics of RIP were presented in [16-20]. These studies focus on swing-up control [15,21], stabilization control [15,19,20], switching control [23] and trajectory tracking control [24,25]. The RIP is unstable when the position of pendulum in vertical upright, and in a stable condition when the pendulum is in vertically down position [21].

To optimize the stabilization energy, this manuscript proposes a Linear Quadratic regulator (LQR) to tune the feedback gain K in the stabilization law $u=-Kx$. This approach has been widely used in conventional inverted pendulum [20], load frequency control for power system [26], suspension system [27], wind turbine system [28] and in other fields of studies. The rest of the manuscript discusses the dynamic of a rotary inverted pendulum, regulator design methodology that consists of judicious pole placement in full-state-feedback (FSF) and an LQR. Lastly, the comparative performances between FSF and LQR are discussed before the concluding remark.

2. Rotary Inverted Pendulum

RIP embodies a rigid shaft called a pendulum that rotates freely in a vertical plane with the purpose of swinging up and balancing the pendulum in the inverted position. Then, the pendulum is bound to a pivot arm that is installed on the shaft of the servomotor. Therefore, the pivot arm can be rotated in the horizontal plane by the servomotor while the pendulum is hanging downward. On the contrary, the optical encoders are installed on the pivot arm and pendulum arm to identify the displacement of the RIP system. Fig.1 shows the structure of the RIP system.

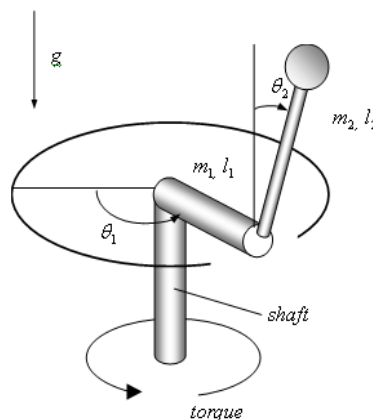


Fig. 1 Simplified rotary inverted pendulum schematic [22]

The numerical values of the mechanical and electrical system parameters for the RIP system are provided in Table 1. Whereas Table 2 tabulates the numerical nomenclature of the RIP system.

Table 1 RIP system variables and parameters

Parameters	Description
m_1	Mass of arm
m_2	Mass of pendulum
l_1	Length of arm
l_2	Length of pendulum
c_1	Distance to the center of mass of arm
c_2	Distance to the center of mass of pendulum
J_1	Inertia of arm
J_2	Inertia of pendulum
θ_1	Angular displacement of arm
$\dot{\theta}_1$	Angular velocity of arm
θ_2	Angular displacement of pendulum
$\dot{\theta}_2$	Angular velocity of pendulum
τ_1	Applied torque
g	Gravitational acceleration

Table 2 The numerical values of the mechanical and electrical system parameters

Physical Quantity	Symbol	Numerical Value
Mass of Arm	m_1	0.056 kg
Length of Arm	l_1	0.16 m
Distance to Arm Center of Mass	c_1	0.08 m
Inertia of Arm	J_1	0.00215058kg-m ²
Mass of Pendulum	m_2	0.022 kg
Length of Pendulum	l_2	0.16 m
Distance To Pendulum Center of Mass	c_2	0.08 m
Inertia of Pendulum	J_2	0.00018773 kg-m ²
Armature Resistance	R_m	2.5604 Ω
Back-emf Constant	K_b	0.01826 V-s/rad
Torque Constant	K_t	0.01826 N-m/A

Modeling the RIP is an established method, with various analytical approaches appearing in the previous research [29, 30]. To develop a mathematical model of RIP system, let define the angular displacement of the arm and the angular displacement of the pendulum as $q=[\theta_1 \theta_2]^T$. The lumped dynamic (1), (2) and (3) renders the equation of motion of the RIP in Equation (4).

$$M(q) = \begin{bmatrix} J_1 + m_2 l_2^2 + m_2 c_2^2 \sin^2 \theta_2 & m_2 l_1 c_2 \cos \theta_2 \\ m_2 l_1 c_2 \cos \theta_2 & J_2 + m_2 c_2^2 \end{bmatrix} \quad (1)$$

$$V_m(q, \dot{q}) = \begin{bmatrix} \frac{1}{2} m_2 l_1^2 \dot{\theta}_2 \sin^2(2\theta_2) & -m_2 l_1 c_2 \dot{\theta}_2 \sin \theta_2^2 + \frac{1}{2} m_2 c_2^2 \dot{\theta}_1 \sin(2\theta_2) \\ -\frac{1}{2} m_2 c_2 \dot{\theta}_1 \cos(2\theta_2) & 0 \end{bmatrix} \quad (2)$$

$$G(q) = \begin{bmatrix} 0 \\ -m_2 c_2 g \sin \theta_2 \end{bmatrix} \quad (3)$$

$$M(q)\ddot{q} + V_m(q, \dot{q})\dot{q} + G(q) = \begin{bmatrix} \tau_1 \\ 0 \end{bmatrix} \quad (4)$$

The voltage signal to the servomotor is controlled by a PWM driver. The duty cycle is decided by a control law generated on the control side. As such, there exists a linear relationship between the control torque and the control voltage e as in Equation (5)

$$\tau_1 = \frac{K_b}{R_m} e - \frac{K_b^2}{R_m} \dot{\theta}_1 \quad (5)$$

By defining a state variables $[X_1 \ X_2 \ X_3 \ X_4]^T = [\theta_1 \ \theta_2 \ \theta_1 \ \theta_2]$, the derivative of states are

$$\dot{x}_1 = X_3 \quad (6)$$

$$\dot{x}_2 = X_4 \quad (7)$$

$$\dot{x}_3 = \frac{-0.5 \sin 2X_2}{\Delta} (P_2 P_4 X_4^2 + P_4 P_5 X_3 X_4 + P_2 P_3 X_3^2 \cos X_2 + P_3 P_6) - \frac{0.5 P_4}{\Delta} (-2 P_3 X_4^2 \sin X_2 + 2 P_7 X_3 - 2 P_8) \quad (8)$$

$$\begin{aligned} \dot{x}_4 = & \frac{-0.5 \sin 2X_2}{\Delta} (-P_3^2 X_4^2 + P_2 P_3 X_4^2 \cos X_2 + P_3 P_5 X_3 X_4 \cos X_2 + P_1 P_2 X_3^2 \\ & + P_2^2 X_3^2 \sin 2X_2) - \frac{\cos X_2}{\Delta} (P_3 P_7 X_3 - P_3 P_8 u) \pm \frac{P_6 \sin X_2}{\Delta} (P_1 \\ & - P_2^2 \sin X_2) \end{aligned} \quad (9)$$

Note that

$$\Delta = P_1 P_4 + P_2^2 \sin X_2 - P_3^2 \cos^2 X_2 \quad (10)$$

and newly define parameters, P_n as:

$$P_1 = m_2 l_1^2 + J_1, P_2 = m_2 c_2^2, P_3 = m_2 l_1 c_2, P_4 = m_2 c_2^2 + J_2, P_5 = m_2 l_1^2, P_6 = m_2 c_2 g, P_7 = \frac{K_b^2}{R_m}, P_8 = \frac{K_t}{R_m}. \quad (11)$$

Equation (6) - (9) can be linearized by considering the equilibrium state of the system, or by Jacobian [29]. Assume that the angular velocity of the pendulum is too small, that is; $\theta_2 \approx 0$. As such, when the inverted pendulum is near the equilibrium point, $\sin \theta_2 \approx \theta_2$ and $\cos \theta_2 \approx 1$, rendering $(\theta_2) \theta_2 \approx 0$. That is, linearizable condition yields the RIP dynamics in Equations (12), (13), (14), (15).

$$\dot{x}_1 = X_3 \quad (12)$$

$$\dot{x}_2 = X_4 \quad (13)$$

$$\dot{x}_3 = \frac{(m_2 c_2^2 + J_1) \frac{K_t}{R_m} u - m_2^2 c_2^2 l_1 g X_2 - (m_2 c_2^2 + J_2) \frac{K_b K_t}{R_m} X_3}{(m_2 l_1^2 + J_1)(m_2 c_2^2 + J_2) - m_2^2 l_1^2 c_2^2} \quad (14)$$

$$\dot{x}_4 = \frac{-m_2 l_1 c_2 \frac{K_t}{R_m} u + (m_2 l_1^2 + J_1) m_2 c_2 l_1 g X_2 + m_2 l_1 c_2 \frac{K_b K_t}{R_m} X_3}{(m_1 l_1^2 + J_1)(m_2 c_2^2 + J_2) - m_2^2 l_1^2 c_2^2} \quad (15)$$

Plugging in the numerical nomenclature from Table 2 renders a numerical RIP dynamic as in Equations (16)-(17). States x_1 denotes the arm angle, x_2 defines the pendulum angle, and x_3 defines the pendulum angle.

$$\begin{bmatrix} \dot{x}_1 \\ \dot{x}_2 \\ \dot{x}_3 \\ \dot{x}_4 \end{bmatrix} = \begin{bmatrix} 0 & 0 & 1 & 0 \\ 0 & 0 & 0 & 1 \\ 0 & -5.9796 & -0.0527 & 0 \\ 0 & 57.6254 & 0.0451 & 0 \end{bmatrix} \begin{bmatrix} X_1 \\ X_2 \\ X_3 \\ X_4 \end{bmatrix} + \begin{bmatrix} 0 \\ 0 \\ 2.8844 \\ -2.4724 \end{bmatrix} u \quad (16)$$

$$y = [0 \quad 1 \quad 0 \quad 0] \begin{bmatrix} X_1 \\ X_2 \\ X_3 \\ X_4 \end{bmatrix} \quad (17)$$

3. Formulation of The Regulator

The controllability of RIP must be observed to confirm the necessity of the feedback law for stabilization. RIP in a standard state space $\dot{x}=Ax+Bu$ with the output equation $y=Cx$. The controllability of the RIP is substantial in order to assure the possibility of driving the state of the system everywhere in the stability region. The controllability of the RIP can be tested via the controllability matrix $C_m=[B \ AB \ \dots \ A^{n-1}B]$ such that C_m has the rank with the same size of system A . With a numerical formulation, the controllability matrix can be computed as in Equation (18). That is, C_m has rank 4 confirming that the RIP is completely controllable.

$$C_m = \begin{bmatrix} 0 & 2.8844 & -0.1519 & 14.7917 \\ 0 & -2.4724 & 0.1302 & -142.4777 \\ 2.8844 & -0.1519 & 14.7917 & -1.5577 \\ -2.4724 & 0.1302 & -142.4777 & 8.1714 \end{bmatrix} \quad (18)$$

For the RIP system, there exists a feedback control law $u(t)=-Kx(t)$ with a feedback gain K . The design problem is to formulate a gain K such that the closed-loop poles (or eigenvalues) are located on the left-hand side of the S-plane, and hence the closed-loop system $A_{CL} = A - BK$ is known to be stable. Therefore, a judicious choice of the gain K is crucial, such that the control energy $u(t)$ has enough energy to force the system's poles to the stability region. In a full-state-feedback (FSF) approach, the desired closed-loop eigenvalues are pre-defined by the designer using pole placement. The design scheme is conducted by examining the characteristic equation of the closed-loop system $|sI-A_{CL}| = 0$ where the closed-loop dynamic is expressed as $A_{CL} = A - Bu(t)$. For the system at hand, the desired closed-loop pole locations are selected at $P = [-2+j \ -2-j \ -5+j3 \ -5-j3]$. As a result, the feedback gain K is computed as in Equation (19).

$$K = [-1.1226 \ -56.5708 \ -1.2465 \ -7.0956] \quad (19)$$

With FSF-pole placement, the trajectory of arm angle and pendulum angle upon initial condition $X = [1 \ 1 \ 0 \ 0]^T$ is depicted in Fig. 2. The trajectory shows that the RIP can be stabilized within 3 seconds after the perturbation occurs.

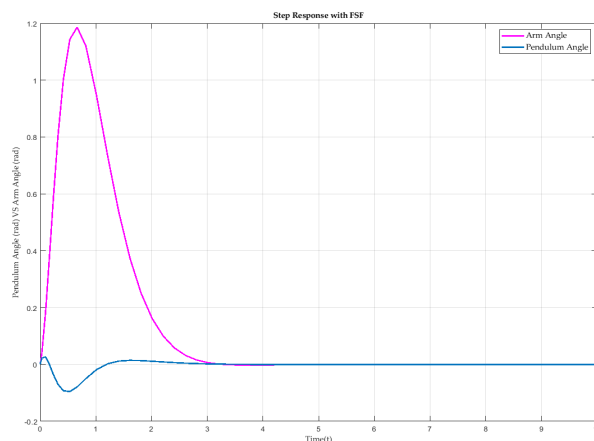


Fig. 2 Arm and pendulum angle trajectory with FSF facility

It is proven that the RIP system is stabilizable by a simple FSF with judicious selection of the desired closed-loop poles location. However, it is interesting to further design the feedback gains at minimum cost that is; achieving stabilization and state regulation with a minimum control energy. To this end, LQR is proposed as a computationally efficient state regulation that produces a minimum control energy. LQR, as an optimal energy-like regulator, provides robust stability with a minimized energy-like performance index. In the LQR methodology, the symmetric and positive definite matrices Q and R are chosen to suit the Lyapunov and Riccati equations. The objective of the LQR is to compute the feedback gain matrix K_{LQR} that minimizes the quadratic cost function J_{LQR} given in (20) to keep the pendulum stable.

$$J_{LQR} = \int_{t_0}^{t_f} (X^T Q X + U^T R U) dt \tag{20}$$

Matrices Q and R affect the overall performance of the system. In this study, three different values of Q are tested to determine the most optimal stabilization. With $R=1$, the three Q -value are depicted in Equation (21).

$$Q_1 = \begin{bmatrix} 1 & 0 & 0 & 0 \\ 0 & 1 & 0 & 0 \\ 0 & 0 & 1 & 0 \\ 0 & 0 & 0 & 1 \end{bmatrix}, \quad Q_2 = \begin{bmatrix} 15 & 0 & 0 & 0 \\ 0 & 1 & 0 & 0 \\ 0 & 0 & 1 & 0 \\ 0 & 0 & 0 & 1 \end{bmatrix}, \quad Q_3 = \begin{bmatrix} 100 & 0 & 0 & 0 \\ 0 & 20 & 0 & 0 \\ 0 & 0 & 10 & 0 \\ 0 & 0 & 0 & 1 \end{bmatrix} \tag{21}$$

Respectively, the optimized gain K_{LQR} that has been produced by positive definite matrices $Q_1, Q_2,$ and Q_3 are expressed in Equation (22), (23) and (24).

$$K_1 = [-0.9906 \ -70.2929 \ -1.5998 \ -9.4630] \tag{22}$$

$$K_2 = [-3.8333 \ -87.4062 \ -3.0187 \ -11.8154] \tag{23}$$

$$K_3 = [-9.8672 \ -137.6378 \ -6.8427 \ -18.7247] \tag{24}$$

4. Result and Discussion

To observe the effectiveness of LQR on the RIP system, the procedure was implemented in SIMULINK through the MATLAB platform. Fig. 3 shows the trajectory of arm angle and pendulum angle with different Q -values. Table 3 tabulates the transient behavior of the RIP during stabilization. The selected transient performances such as settling time, rise time, and peak values are recorded therein. While the overshooting amount can be observed in Fig. 3.

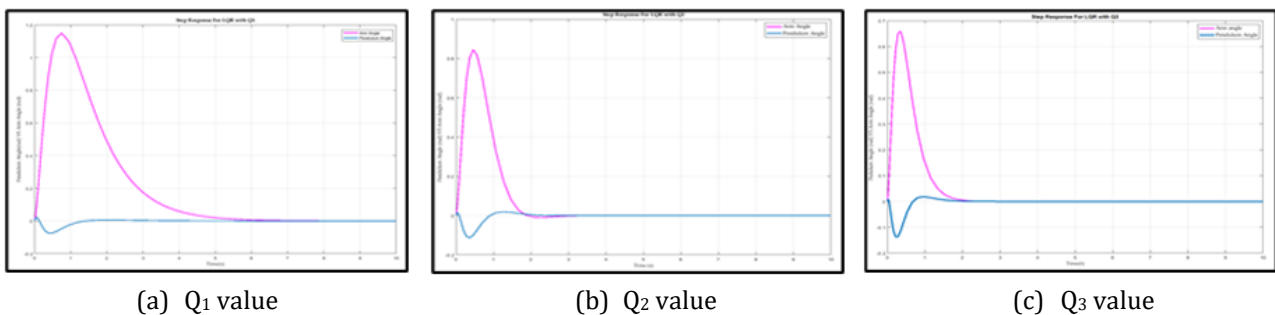


Fig. 3 Trajectory of arm angle and pendulum angle

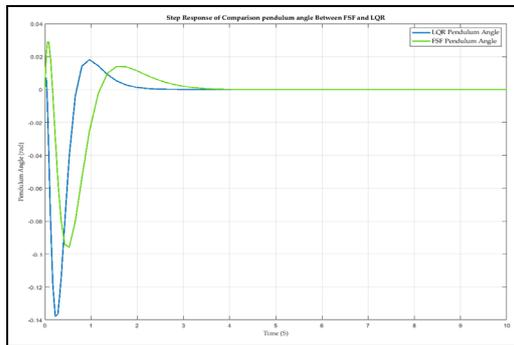
With Q_3 , the regulation time for the pendulum angle is 22.14% faster than the system with Q_2 , and 39.10% faster than the system with Q_1 . The arm angle can be stabilized faster with Q_3 . That is, 16.20% and 56.04% faster than Q_2 and Q_1 respectively. Hence, it can be deduced that a larger Q renders fast stabilization speed. Hence, the pendulum requires a shorter time to be balanced. However, a greater weighting matrix Q makes the pendulum

and the arm overshoot post-stability. This phenomenon can be observed in Table 3 where the pendulum angle and the arm angle peaked at 0.0799 rad and 0.6595 rad, respectively.

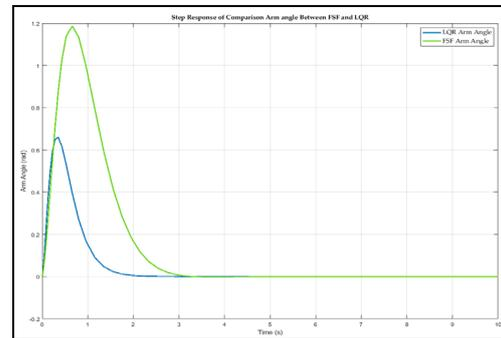
The matrix Q in the cost function in Equation (20) appears in the state regulation problem. The matrix Q must be symmetric and positive-definite. That is, it must have an identical transpose matrix element. As such, the larger Q results in a large outcome when multiplied with the states of the RIP, resulting in fast regulation due to the large stabilizing energy. Whereas matrix R appears in the minimum energy problem, which compromises with the amount of energy required to stabilize the RIP. Fig. 4 indicates the transient history of the pendulum and the arm angle after FSF and LQR. The quantitative performances of both approaches are tabulated in Table 4. Visual observation shows that LQR stabilizes the pendulum cum arm faster as compared to FSF. Quantitatively, data from Table 4 portrays that LQR is able to produce almost 33.87% faster regulation time than FSF. Whereas the arm angle for the RIP system using LQR is stabilized at 28.31% faster than FSF.

Table 3 Pendulum and arm angle with respect to weighing matrix

Weighing Matrix	Q_1		Q_2		Q_3	
Controlled parameter	Pendulum Angle (rad)	Arm Angle (rad)	Pendulum Angle (rad)	Arm Angle (rad)	Pendulum Angle (rad)	Arm Angle (rad)
Rise Time (s)	0.0751	0.7509	0.0313	0.4525	0.2230	0.3507
Settling Time (s)	4.7510	8.3510	3.2630	3.2630	2.0800	2.3530
Peak value	0.0208	1.1490	0.0161	0.8448	0.0799	0.6595



(a) Pendulum Angle



(b) Arm Angle

Fig. 4 Trajectory of arm angle and pendulum angle after FSF and LQR

Table 4 Comparisons of controllers based on simulation result

Tuning method	FSF		LQR	
Controlled parameter	Pendulum Angle (rad)	Arm Angle (rad)	Pendulum Angle (rad)	Arm Angle (rad)
Rise Time (s)	0.0971	0.6637	0.2230	0.3507
Settling Time (s)	4.2110	4.2110	2.0800	2.3530
Peak Value	0.0264	1.1860	0.0799	0.6595

5. Conclusion

From the observation, it can be concluded that LQR exhibits a faster stabilization speed than FSF. However, LQR shows unappealing pendulum angle overshoot post-stability, where the pendulum angle peaked at 0.0799 radian, which is higher than the FSF (0.0264 radian). Arm angle shows appealing performance as it peaked at 0.6595 radian, which is lower as compared to FSF (1.1860 radian). The necessary and sufficient condition for arbitrary and judicious pole placement in FSF is that the system be completely state-controllable. As such, the energy required to push the poles to a new location is proportional to the feedback gain parameter, and in some cases, the energy may peak at a non-practical value. In the LQR, energy is optimized by the cost function, while at the same time, stability is preserved. The use of RIP as a testbed is a challenging task as it is one of the most known unstable and under actuated models available to test the efficacy and effectiveness of the control techniques. For further research, one would suggest the augmentation of artificial intelligence tuning or heuristic techniques for better performance results.

Acknowledgement

This research was developed under the research facilities in the Faculty of Electrical Technology and Engineering, Universiti Teknikal Malaysia Melaka. A special acknowledgement is addressed to the Center for Robotics and Industrial Automation (CeRIA), and the Ministry of Education, Malaysia.

Conflict of Interest

Authors declare that there is no conflict of interests regarding the publication of the paper.

Author Contribution

The authors confirm contribution to the paper as follows: **Formulation of Dynamical model of RIP:** Muhammd Nizam Kamarudin; **Literature survey and review:** Rozilawati Mohd Nor; **Formulation of FSF with Simulation analysis:** Sahazati Md Rozali; **Formulation of LQR with Simulation analysis:** Muhammad Nizam Kamarudin; **draft manuscript preparation:** Muhammad Nizam Kamarudin, Mohd Saifuzam Jamri. All authors reviewed the results and approved the final version of the manuscript.

References

- [1] Iswanto, Nia Maharani Raharja, Alfian Ma'arif, Yogi Ramadhan & Phisca Aditya Rosyady (2021) Pole Placement Based State Feedback for DC Motor Position Control, *Journal of Physics: Conf. Ser.*, 17(83), pp. 1–7, <https://doi.org/10.1088/1742-6596/1783/1/012057>
- [2] Varun Gupta, Vineet Gupta, Anurag Shukla, & N. Sukavanam (2019) State Feedback controller design using Pole-placement method and its implementation using MATLAB. *International Journal of Applied Engineering Research*, Vol.14(2), pp. 145–150, <http://www.ripublication.com>
- [3] Thomas Chaffre, Gilles Le Chenadec, Karl Sammut, Estelle Chauveau, & Benoit Clement (2021) Direct Adaptive Pole-placement Controller using Deep Reinforcement Learning: Application to AUV Control, *ScienceDirect IFAC papersOnline*, Vol. 54(16), pp. 333–340, <https://doi.org/10.1016/j.ifacol.2021.10.113>
- [4] Neelu Nagpal, Vijyant Agarwal, & Bharat Bhushan (2018) A Real-Time State-Observer-Based Controller for a Stochastic Robotic Manipulator, *IEEE Transactions On Industry Applications*, Vol. 54 (2), pp. 1806–1822, <https://doi.org/10.1109/TIA.2017.2785339>
- [5] Inthamoussou, F. A., Bianchi, F. D., Battista, H. D. & Mantz, R. J. (2014) LPV Wind turbine control with anti-windup features covering the complete wind speed range, *IEEE Transaction on Energy Conversion*, Vol. 29(1), pp. 259–266, <https://doi.org/10.1109/TEC.2013.2294212>
- [6] Meisami-Azad, M., Mohammadpour, J. and Grigoriadis, K. (2012) *Anti-windup LPV control of pitch actuators in wind turbines*. American Control Conference (ACC), Fairmont Queen Elizabeth, Montreal, QC, pp. 6801–6808, <https://doi.org/10.1109/ACC.2012.6315468>
- [7] Eun, Y., Gökçek, G., Kabamba, P. T. & Merkov, S. M. (2002) *An LQG approach to systems with saturating actuators and anti-windup implementation*, IFAC Proceedings Volumes, Vol. 35(1), pp. 91–96, <https://doi.org/10.3182/20020721-6-ES-1901.01086>
- [8] Huang Da, Huang ShuCai. (2018) *Optimal controller design based on minimum principle*. SMIMA MATEC Web of Conferences 173, <https://doi.org/10.1051/mateconf/20180100101001>
- [9] Baranov, L. A., Meleshin, I. S., & Trinh, L. M. 2011 Optimal Control of a Subway Train with Regard to the Criteria of Minimum Energy Consumption, *Russian Electrical Engineering*, Vol. 82 (8), pp. 405–410, <https://link.springer.com/article/10.3103/S1068371211080049>
- [10] Dionisis Stefanatos & Jr-Shin Li (2010) Constrained minimum-energy optimal control of the dissipative Bloch equations. *Systems and Control Letters*. Vol.59(10), pp. 601–607, <https://doi.org/10.1016/j.sysconle.2010.07.004>
- [11] Sang-Young Oh & Ho-Lim Choi (2021) Regulation of a Class of Nonlinear Systems with Unknown Growth Rate Under Uncertain Measurement Sensitivity, *Journal of Electrical Engineering & Technology*, Vol.16(5), pp. 2767–2775, <https://doi.org/10.1007/s42835-021-00826-1>
- [12] Muhssin, M.T., Ajaweed, M.N. & Khalaf, S.K. (2023) Optimal control of underwater vehicle using LQR controller driven by new matrix decision control algorithm, *International Journal of Dynamics and Control*, Vol. 11, pp. 2911–2923, <https://doi.org/10.1007/s40435-023-01186-6>
- [13] M. Nizam Kamarudin, S. Md. Rozali & A. Rashid Husain (2013) Observer-Based Output Feedback Control with Linear Quadratic Performance, *Procedia Engineering*, Vol.53, pp. 233–240, <https://doi.org/10.1016/j.proeng.2013.02.031>
- [14] M. Amin Sharifi K. (2010). Design, build and control of a single rotational inverted pendulum. [Graduate dissertation, University of Tehran, Iran]. <https://api.semanticscholar.org/CorpusID:16014516>

- [15] Mathew, N. J., Rao, K. K., & Sivakumaran, N. (2013) Swing up and stabilization control of a rotary inverted pendulum. *The 10th IFAC International Symposium on Dynamics and Control of Process Systems*, The International Federation of Automatic Control, Mumbai, India, pp. 654–659, <https://doi.org/10.3182/20131218-3-IN-2045.00128>
- [16] Hamza, M. F., Yap, H. J., Choudhury, I. A., Isa, A. I., Zimit, A. Y., & Kumbasar, T. (2019) Current development on using Rotary Inverted Pendulum as a benchmark for testing linear and nonlinear control algorithms, *Mechanical Systems and Signal Processing*, 116, pp. 347–369, <https://doi.org/10.1016/j.ymssp.2018.06.054>
- [17] Dwivedi, P., Pandey, S., & Junghare, A. (2017) Performance Analysis and Experimental Validation of 2-DOF Fractional-Order Controller for Underactuated Rotary Inverted Pendulum, *Arabian Journal for Science and Engineering*, Vol. 42(12), pp. 5121–5145, <https://doi.org/10.1007/s13369-017-2618-8>
- [18] Hamza, M. F., Yap, H. J., & Choudhury, I. A. (2015) Genetic Algorithm and Particle Swarm Optimization Based Cascade Interval Type 2 Fuzzy PD Controller for Rotary Inverted Pendulum System, *Mathematical Problems in Engineering*, Hindawi, Vol. 2015, <https://doi.org/10.1155/2015/695965>
- [19] Kumar, P., & Mukherjee, R. (2013) Modelling and Controller Design of Inverted Pendulum, *International Journal of Advanced Research in Computer Engineering & Technology*, Vol. 2(1), pp. 200–206.
- [20] Sirisha, V., & S. Junghare, A. (2014) A Comparative study of controllers for stabilizing a Rotary Inverted Pendulum, *International Journal of Chaos, Control, Modelling and Simulation*, Vol.3(1/2), pp. 1–13, <https://doi.org/10.5121/IJCCMS.2014.3201>
- [21] Akhtaruzzaman, M., & Shafie, A. A. (2010) *Modeling and control of a rotary inverted pendulum using various methods, comparative assessment and result analysis*, IEEE International Conference on Mechatronics and Automation, ICMA 2010, Xi'an, China, pp. 1342–1347, <https://doi.org/10.1109/ICMA.2010.5589450>
- [22] Shojaei, A. A., Othman, M. F., Rahmani, R., & Rani, M. R. (2011) *A hybrid control scheme for a rotational inverted pendulum*, 2011 UKSim 5th European Symposium on Computer Modeling and Simulation, Madrid, Spain, pp. 83–87, <https://doi.org/10.1109/EMS.2011.79>
- [23] Hamza, M.F., Yap, H.J., Choudhury, I.A., Isa, A.I., Zimit, A.Y. & Kumbasar, T. (2019) Current development on using Rotary Inverted Pendulum as a benchmark for testing linear and nonlinear control algorithms, *Mechanical Systems and Signal Processing*, Vol.116, pp. 347–369, <https://doi.org/10.1016/j.ymssp.2018.06.054>
- [24] Yue, M., Wang, S. & Sun, J.Z. (2016) Simultaneous balancing and trajectory tracking control for two-wheeled inverted pendulum vehicles: A composite control approach. *Neurocomputing*, Vol. 191, pp. 44–54, <https://doi.org/10.1016/j.neucom.2016.01.008>
- [25] Yue, M., An, C. & Sun, J.Z. (2018) An efficient model predictive control for trajectory tracking of wheeled inverted pendulum vehicles with various physical constraints, *International Journal of Control, Automation and Systems*, Vol. 16(1), pp. 265–274, <https://link.springer.com/article/10.1007/s12555-016-0393-z>
- [26] Shaharudin, N., Kamarudin, M.N., Hairi, M.H. & Rizman, Z.I. (2018) Achieving Power System Stability for Two Area Hydro Power System via LQR Techniques, *International Journal of Engineering and Technology*, Vol. 7, pp.396–402, <https://doi.org/10.14419/ijet.v7i3.14.18825>
- [27] Bharali, J. & Buragohain, M. (2016) *Design and performance analysis of fuzzy LQR; fuzzy PID and LQR controller for active suspension system using 3 degree of freedom quarter car model*, IEEE 1st International Conference on Power Electronics, Intelligent Control and Energy Systems (ICPEICES), Delhi, India, pp. 1–6, <https://doi.org/10.1109/ICPEICES.2016.7853369>
- [28] Kamarudin, M.N., Husain, A.R. & Ahmad, M.N. (2014) Variable speed wind turbine with external stiffness and rotor deviation observer, *Applied Mechanics and Materials*, Vol. 661, pp. 154–159, <https://doi.org/10.4028/www.scientific.net/AMM.661.154>
- [29] Abdulrahman H. Bajodah, Uzair Ansari (2023) Rotary Inverted Pendulum Control using Robust Generalized Dynamic Inversion with Adaptive Neural Estimation, *ScienceDirect IFAC papersOnline*, Vol. 56(2), pp. 10570–10575, <https://doi.org/10.1016/j.ifacol.2023.10.675>
- [30] Shishir Patil, Uma Kulkarni, Aditya Ingale & Rakesh Halligudi (2022) *Rotary Inverted Pendulum-Stability Assessment*, IEEE 2nd Mysore Sub Section International Conference (MysuruCon), Mysuru, India, pp. 1–5, <https://doi.org/10.1109/MysuruCon55714.2022.9972380>
- [31] Muhammad Nizam Kamarudin, Sahazati Md. Rozali, Mohd Hendra Hairi, Alias Khamis, & Abdul Rashid Husain (2019) Linearization - Advantages and Shortcomings Toward Control System Design, *International Journal of Electrical Engineering and Applied Sciences*, Vol. 29(2), pp. 17–21, <https://ijeeas.utm.edu.my/ijeeas/article/view/5073>